Potassium-based sorbents using mesostructured γ-alumina supports for low temperature CO_2 capture

M.B. Durán-Guevara[a], J. Ortiz-Landeros[b,*], H. Pfeiffer[c],
M.I. Espitia-Cabrera[d], M.E. Contreras-García[a,*]

[a]*Instituto de Investigaciones Metalúrgicas, Edificio "U", Ciudad Universitaria, Universidad Michoacana de San Nicolás de Hidalgo,
CP 58060, Morelia, Michoacán, Mexico*
[b]*Departamento de Ingeniería en Metalurgia y Materiales, Escuela Superior de Ingeniería Química e Industrias Extractivas, IPN, UPALM,
Av. Instituto Politécnico Nacional s/n, CP 07738, México DF, Mexico*
[c]*Instituto de Investigaciones en Materiales, Universidad Nacional Autónoma de México, Circuito exterior s/n, Cd Universitaria, Del. Coyoacán,
CP 04510, México DF, Mexico*
[d]*Facultad de Ingeniería Química, Edificio "M", Ciudad Universitaria, Universidad Michoacana de San Nicolás de Hidalgo,
CP 58060, Morelia, Michoacán, Mexico*

Abstract

In this work, a series of mesoporous alumina materials exhibiting high surface areas have been synthesized, characterized and used in the preparation of CO_2 sorbents. The mesostructured powders were prepared through a soft chemistry route, employing aluminum tri-sec-butoxide-derived sol precursors in the presence of different surfactants. Structural and microstructural characterization techniques showed that γ-Al_2O_3 powders were composed of nanocrystals, and the samples presented high surface area values (238.6–496.7 $m^2 g^{-1}$) produced by a high mesostructured order, depending on the surfactant used as structure-directing agent.

Based on the textural features, selected γ-Al_2O_3 materials were employed as supports for the preparation of potassium-based sorbents for CO_2 capture at low temperatures (30–80 °C). Potassium-loaded alumina supports were synthesized by a wet impregnation method, and the CO_2 sorption tests were conducted via thermogravimetric analysis. The surface area and pore volume of the potassium-impregnated supports experienced a noticeable reduction, in comparison with the original values, suggesting the inclusion of potassium inside the support porosity. Nevertheless, the sorbents showed excellent reactivity; in fact, the potassium/γ-Al_2O_3 sorbent prepared with 40 wt% potassium content had a maximum CO_2 capture capacity of 4.03 mmol CO_2/g sorbent at the relatively low temperature of 80 °C in the presence of water vapor. These results suggest that both the potassium content and textural properties of mesostructured γ-Al_2O_3 supports could provide an enhancement of the CO_2 absorption properties.

1. Introduction

Due to the direct connection between the emissions of anthropogenic greenhouse gases, such as carbon dioxide, and the current environmental issues of global warming, there is a growing interest in the development of new technologies for the control and gradual mitigation of these types of pollutant emissions [1–3]. A good example of this is the intense research focused on the study of solid sorbents for the chemical absorption of CO_2 [4–11].

The use of solid sorbents based on alkaline and alkaline-earth ceramics has been reported in many studies as a promising option
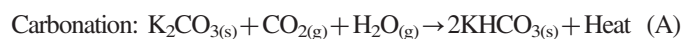
*Corresponding authors. Tel.: +52 5557296000x54267; fax: 5557254267.
E-mail addresses: jortizla@ipn.mx (J. Ortiz-Landeros),
eucontre@gmail.com (M.E. Contreras-García).

for CO_2 capture [12]. Depending on the properties of the materials, the solid sorbents are able to selectively trap CO_2 within a wide range of temperatures and CO_2 concentrations; because of the adsorption/desorption capability, there is the additional option for the subsequent catalytic chemical conversion of CO_2 into value-added products [13].

Regarding K_2CO_3-based solid sorbents, reported studies suggest that these materials could be applied to chemically capture CO_2 at low absorption temperatures ranging from room temperature to 90 °C, with thermal regeneration at temperatures of 150–400 °C during multiple cycles [14–17]. Thanks to such regeneration characteristics, these particular solid sorbents are an attractive option, compared with other low temperature sorbents, such as aqueous solutions of NaOH, KOH and CaOH that involve multi-stage and energy-intensive processes in the regeneration step [17–20].
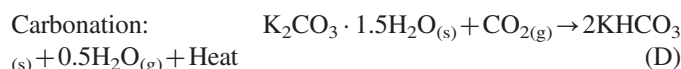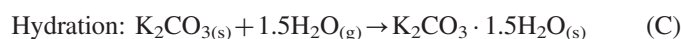
The CO_2 capture process using K_2CO_3-based sorbents under moist conditions involves the reactions of carbonation and regeneration, as follows [14,21]:

Carbonation: $K_2CO_{3(s)} + CO_{2(g)} + H_2O_{(g)} \rightarrow 2KHCO_{3(s)} + Heat$ (A)

$\Delta H_{60\,°C} = -143\ kJ\ mol^{-1}$

Regeneration: $2KHCO_{3(s)} \rightarrow K_2CO_{3(s)} + CO_{2(g)} + H_2O_{(g)}$ (B)

The formation of intermediate potassium-containing species in the presence of water vapor at temperatures between 50 and 70 °C has also been reported, and they are subsequently prone to react with CO_2 as follows:

Hydration: $K_2CO_{3(s)} + 1.5H_2O_{(g)} \rightarrow K_2CO_3 \cdot 1.5H_2O_{(s)}$ (C)

Carbonation: $K_2CO_3 \cdot 1.5H_2O_{(s)} + CO_{2(g)} \rightarrow 2KHCO_{3(s)} + 0.5H_2O_{(g)} + Heat$ (D)

$\Delta H_{60\,°C} = -44\ kJ\ mol^{-1}$

Energy consumption could be reduced if the heat released during carbonation reactions and its possible use during the regeneration stage is taken into consideration [21].

Several studies regarding the design of K_2CO_3 and other alkaline-based sorbents have shown the crucial role that the sorbent support plays in both the absorption and regeneration stages [22–25]. For instance, depending on the nature of the supports, the active phase (K_2CO_3) could be homogeneously dispersed on the support surface, resulting in a significant increase in reactivity during absorption; therefore, a consequent increase in the final absorption kinetics. In addition, some studies have shown that reactivity between the active phase and the support must be avoided. Soo Chool Lee et al. [25,29] studied the CO_2 absorption properties of different K_2CO_3-based sorbents prepared by using several porous materials as supports, such as activated carbon, TiO_2, MgO, Al_2O_3 and SiO_2, as well as some zeolite-type materials. They successfully performed both the CO_2 absorption and regeneration processes in the presence of water vapor. The best results in terms of net sorption capacity and regeneration at low temperatures were observed in the cases of activated carbon and TiO_2. On the other hand, the results showed that when other supports such as MgO were used, the capture capacity decreased after only two cycles. The authors concluded that the reason for this behavior was the formation of certain thermally stable reaction products other than $KHCO_3$, which were not completely reconverted to the original active phase of K_2CO_3 at a low temperature. Based on the above, several other supports, such as Al_2O_3, Y_2O_3, ZrO_2 and mesostructured silica, among others, have been developed to improve the absorption/regeneration performance of K_2CO_3-based solid sorbents [26–29].

Another interesting option for the development of CO_2 sorbents with improved capture properties is the use of mesoporous materials as supports [30]. Various amine-based sorbents showing high CO_2 sorption capacities at low temperatures have recently been obtained by the incorporation of organic amines into mesoporous supports, such as SBA, MCM and other mesostructured silica-based materials [31–33], a silica aerogel [34] and mesoporous carbonaceous materials [35,36].

It is important to mention that despite the substantial progress made in research on CO_2 capture by using dry regenerable solid sorbents, clear limitations and challenges for optimizing the CO_2 absorption performance of these types of materials still exist, especially if the absorption is to be used for large-scale implementation [3]. In this sense, efforts must be directed at obtaining absorbents for CO_2 capture purposes that exhibit the following properties: (1) high absorption capacity and selectivity, (2) high uptake rate, (3) easy regeneration and (4) high stability [37,38]. These improvements can be attained via physical (microstructural) or chemical modification of the sorbent properties though the use of different experimental approaches [39].

In our work, we propose the fabrication and potential application of a series of K_2CO_3-based sorbents supported on mesoporous alumina materials for CO_2 capture at a low temperature. It is assumed that the chemical and thermal stability of the support, in combination with its textural properties, could improve the capture properties of these potassium-based sorbents.

2. Experimental procedure

2.1. Preparation of γ-Al_2O_3 sorbent supports

A series of five mesoporous alumina supports were prepared via the polymeric sol–gel method with surfactant templates. First, a solution of aluminum tri-sec-butoxide ($Al(OC_4H_9)_3$, 97% Aldrich) in 1-Butanol ($CH_3(CH_2)_3OH$ 99.8% Aldrich) with a 1:1 ratio in volume was used as an organic sol precursor. This aluminum solution source was then mixed by stirring it together with the required amount of an aqueous solution of the corresponding surfactant. Four different surfactants were used as templates: cetyltrimethylammonium bromide (CTAB, > 99% Sigma-Aldrich), sodium dodecyl sulfate (SDS, > 98.5% Sigma-Aldrich), Pluronic® F-127 and polyethylene glycol sorbitan monolaurate (Tween® 20). In all of the above cases, the surfactant solutions were prepared with a 1:9 surfactant to water ratio by weight. Another sample was

also prepared without any surfactant addition and was used for comparison purposes.

The resulting sol solution was gelled for 6 h and underwent solvent evaporation at 100 °C in air for 24 h. During these stages, the micellar arrays of the different surfactant templates were self-assembled and the inorganic hydrolyzed precursor polymerized into a metal oxide network. Finally, the as-made samples were calcined at 500 °C for 1 h with a heating rate of $1 \, °C \, min^{-1}$. Based on the surfactant used, the prepared mesostructured alumina samples were labeled as A, A-CTAB, A-SDS, A-Pluronic and A-Tween.

2.2. Preparation of potassium/γ-Al_2O_3 solid sorbents

Potassium-based solid sorbents were obtained via a wet impregnation method. In brief, the different sorbents were prepared by loading 0.30 g of the mesostructured γ-Al_2O_3 (A-Tween sample) with the desired amount of potassium, i.e., 10, 20 or 40 wt%, using 1.0 mL of a KOH aqueous solution with a concentration of 0.95, 2.13 or 5.68 M, respectively. The excess water in the sample was removed in a convection oven by slow evaporation at 80 °C for 24 h. The dried sorbents were then stored in a desiccator until undergoing characterization and CO_2 capture capacity evaluation. The sorbent samples prepared with the different potassium loadings were denoted as A-Tween-10K, A-Tween-20K and A-Tween-40K, in which xK was the weight percentage of the potassium loaded in the sorbent, and A-Tween represented the same support material for all of the cases. Additionally, the A-20K sorbent was prepared by the impregnation of the A support. This sorbent was also tested for comparison purposes.

2.3. Characterization of the solid sorbents

Characterization of the textural properties of both the mesostructured supports and the sorbents was performed through N_2 sorption measurements using a Belsorp-mini II analyzer from BEL Japan. The samples were degassed at 80 °C under vacuum for 24 h. The specific surface area (SSA$_{BET}$) values were obtained from the N_2 adsorption isotherms, using the BET model. The pore volume was calculated on the basis of the amount of adsorbed N_2 after finishing pore condensation at a relative pressure of $P/P_0 = 0.995$. Pore size distribution was determined by the BJH method using the desorption curves.

Structural and microstructural characterization was performed using powder X-ray diffraction and electron microscopy techniques. XRD patterns of both sorbent supports and impregnated sorbents were collected through the use of a Bruker AXS D8 Advance diffractometer; additionally a low angle XRD technique was used to characterize the ordering degree of the mesoporous array of the supports. In this case, the XRD patterns were collected using a Siemens D5000 diffractometer equipped with Co $K\alpha$ radiation ($\lambda = 1.789$ Å). Scanning electron microscopy (SEM) and high-resolution transmission electron microscopy analyses were performed

with a JEOL JSM-6400 microscope and a PHILIPS TECHNAI 200 microscope, respectively.

2.4. CO_2 capture evaluation

The CO_2 sorption capacity was evaluated by thermogravimetric analysis using a TA Instruments Q5000SA thermobalance. In this series of experiments, the sorption tests were performed at temperatures varying from 40 to 80 °C and relative humidity values ranging from 0 to 80% RH. In all of the cases, sorption tests were performed under a 100% CO_2 atmosphere and a temperature heating rate of $1.0 \, °C \, min^{-1}$, from 30 °C to the target temperature.

3. Results and discussion

3.1. Structural, microstructural and physiochemical characterization of supports and impregnated sorbents

The different supports calcined at 500 °C were characterized using XRD, and the results showed the crystalline nature of the support. Fig. 1 shows the XRD pattern of the A-Tween sample. The crystalline γ-Al_2O_3 phase was identified. A diffraction profile can be observed that exhibits broad peaks, suggesting a small crystallite size. All of the reflections correspond to the γ-alumina phase; according to JCPDS card No. 01-079-1558. In addition, the low angle XRD pattern revealed that a certain degree of ordering of the porous structure was obtained. In fact, it is well known that the surfactant template technique offers the possibility of synthesizing ordered mesoporous materials. In this sense, the appearance of the reflections at $2\theta < 5°$ indicated that a certain degree of mesoscopic order was obtained (Fig. 1b).

Transition aluminas obtained by thermal treatment of sol–gel precursors at temperatures between 300 and 600 °C may include γ, θ and δ-Al_2O_3 metastable phases [40], and depending on the starting precursor, γ-Al_2O_3 could be present in cubic, as well as in distorted tetragonal phases [41]. Based on the above findings, further characterization was conducted on a selected A-Tween support by TEM analysis. Fig. 2 shows the high resolution TEM image of the sample. Fig. 2a shows several nanocrystalline domains as straightforward evidence of the crystallinity of the sample, and the nanocrystal in Fig. 2a was indexed; Fig. 2b and c show the obtained TEM diffraction pattern and the high-resolution image, respectively. The recorder electron diffraction pattern had clear diffractions spots, which corroborated the fact that the observed particles were single crystals. Additionally, powder supports were identified as γ-alumina with the face-centered cubic phase. According to the JCPDS card number 01-07-1558, the inter-lattice distances were calculated as follows: $d(3\,1\,1) = 2.29$ Å, $d(4\,0\,0) = 1.99$ Å, $d(6\,2\,0) = 1.26$ Å and $d(4\,4\,0) = 2.38$ Å.

All of the synthesized alumina supports, except the A-SDS support, showed high surface area values and pore size in the mesoporous range. Table 1 shows the textural characteristics of the different samples after thermal treatment at 500 °C. The highest surface area value of $496.7 \, m^2 \, g^{-1}$ corresponded to the
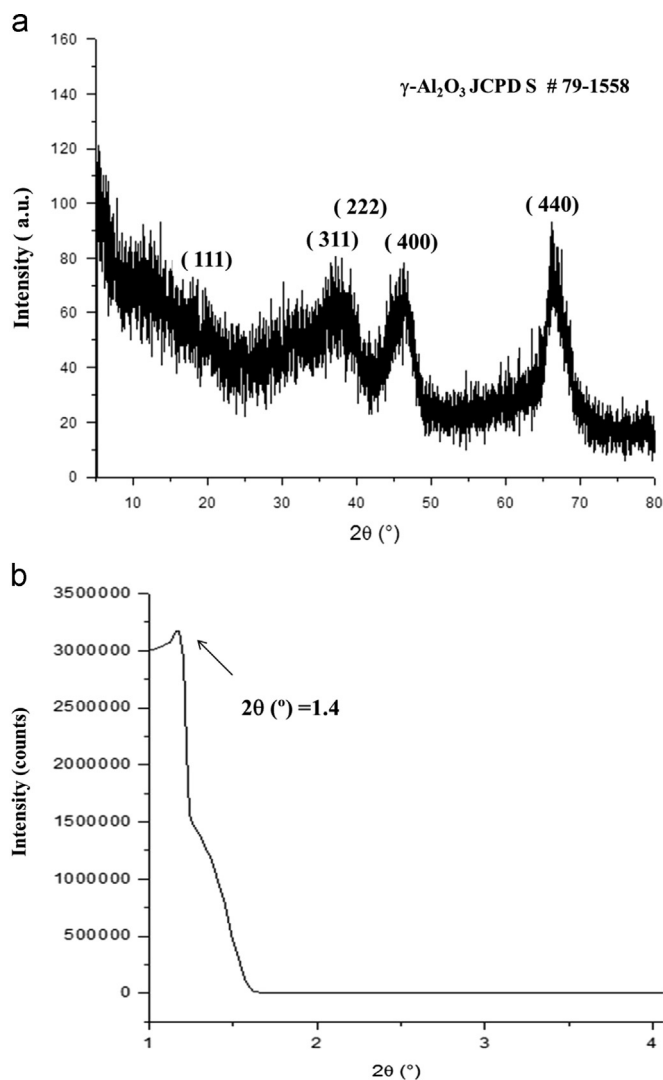
Fig. 1. X-ray diffraction patterns of the A-Tween alumina sample: (a) powder XRD pattern and (b) low angle XRD pattern showing the incipient ordered mesostructure.

A-Tween support and it is evident that only the A-SDS sample exposed a lower surface area value than the sample obtained without using a surfactant template.

Fig. 3 shows the N_2 adsorption/desorption isotherms of the different alumina supports. According to the IUPAC classification [42], samples A, A-Pluronic (Fig. 3a) and A-Tween (Fig. 3b) presented type IV isotherms, which are attributed to mesoporous materials. Isotherms present the characteristic plateau at high P/P_0 that indicates pore filling. These isotherms also show certain differences in the shape of their hysteresis loops, which are correlated with the occurrence of pore condensation, and therefore with the textural features. In contrast to A and A-Pluronic that exhibited H2 hysteresis, the A-Tween support showed an H1-type loop. Once again, based on the IUPAC classification, it is widely accepted that the H1 loop corresponds to mesoporous materials with certain well-defined cylindrical-like pores; this is not the case in H2 hysteresis, in which the distribution of pore size and shape is not well-defined [42]. On the other hand, the A-CTAB (Fig. 3a) and A-SDS (Fig. 3c) supports presented less common sorption

type II isotherms. Hysteresis loops were type H3, and non-stepwise adsorption was observed and interpreted as a result of the presence of slit-like pores.

Fig. 3d shows the estimated pore sizes of the different supports for comparative purposes. As mentioned before, all samples generally presented pore sizes in the mesoporosity range (Table 1). The biggest pore sizes were obtained when the A-Tween surfactant was used. These textural characteristics are important for support applications from the viewpoint that they promote fast mass transport. The differences regarding pore sizes are in accordance with the lengths of the carbon chains of the surfactant templates used; actually, Tween and SDS molecules have the longest and shortest carbon chains, respectively. Additionally, it can be concluded that the low pore volumes and small surface area values observed in the case of the A-SDS supports results because of the collapse of the small mesoporous microstructure due to shrinkage experienced by the gel precursors during calcination.

All of these results suggest the superior textural properties of the A-Tween material when used as the support in sorbent preparation. In fact, these materials were impregnated with different amounts of potassium as the active phase of the sorbent. Table 2 shows the textural features of the different impregnated sorbents. Specific surface area values were estimated by the N_2 adsorption measurements and calculated by applying the BET model. The surface area decreased significantly after impregnation; these noticeable changes in the microstructural features suggest the inclusion of potassium inside the support porosity, which may also result in pore volume filling. In other words, these results suggest the correct incorporation of the potassium active phase in the support, a fact that was confirmed by the EDS microanalysis. Table 2 shows the elemental potassium content on the impregnated sorbents. The obtained potassium loading differed from the nominal values. This suggests that not all of the impregnated potassium remains on the support, but that a certain amount of the active phase is in some way leached out from the support during the sorbent preparation. Regarding these results, it is also important to keep in mind the limitations of the single spot mode microanalysis conducted by the EDS technique. Due to the above, the sorption capacity must be estimated based on the experimentally observed potassium contents.

Prior to CO_2 capture evaluation, the morphology and crystalline phase composition of the prepared sorbents were also characterized by the XRD and SEM techniques. Fig. 4 shows the SEM images of both the bare support and the impregnated samples. The powder supports were made out of submicrometric and spheroidal-like aggregates of nanometric particles, forming an interconnected porous microstructure (Fig. 4a). After impregnation, the powders exhibited larger sizes than the bare supports; the sorbents were actually aggregates of several microns and showed a dense and smooth surface (Fig. 4b and c). These results were in accordance with the surface area values obtained (Table 2).

Generally speaking, XRD analysis of impregnated sorbents showed the presence of both K_2CO_3 and $K_2CO_3 \cdot 1.5H_2O$ supported on the γ-Al_2O_3; both crystalline phases were
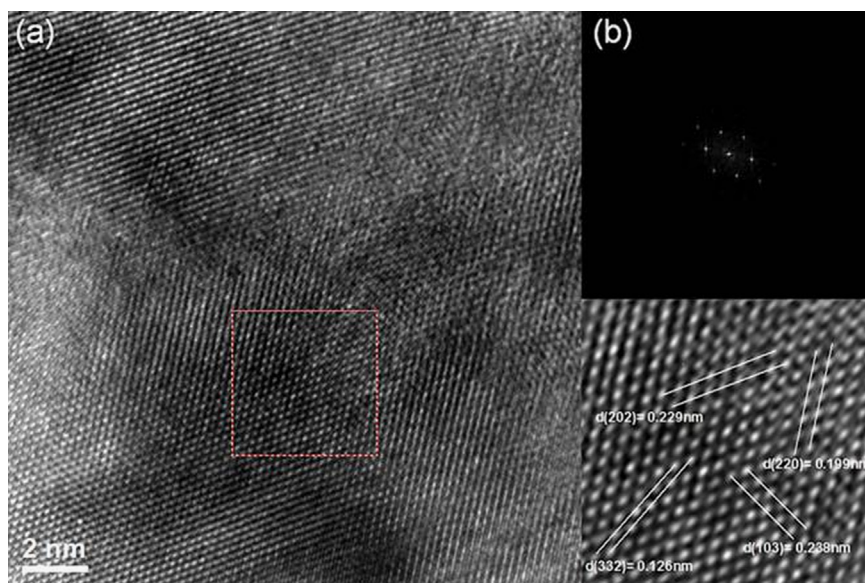
Fig. 2. HRTEM image of A-Tween support showing: (a) the nano-crystalline domains and (b) the characteristic single crystal diffraction pattern.

Table 1
Textural properties of the different mesoporous alumina supports.

Sample	SSA$_{BET}$ (m^2 g^{-1})	Total pore volume[a] (cm^3 g^{-1})	Mean pore diameter[b] (nm)
A	238.6	0.38	2.41
A-Tween	496.7	1.06	7.98
A-Pluronic	300.0	0.72	2.41
A-CTAB	310.3	0.81	1.22
A-SDS	7.5	0.02	2.74

[a]Total pore volume based on N_2 adsorption and $P/P_0 = 0.975$.
[b]Mean pore diameter calculation based on desorption isotherms and the BJH model.

identified in the JCPDS database. For example, Fig. 5 shows the XRD pattern of the A-Tween-40K sorbent. These results suggest that CO_2 capture can subsequently take place through reactions (A) and (D). It is suggested that the formation of the $K_2CO_3 \cdot 1.5H_2O$ active phase was promoted due to the presence of well-distributed KOH in the support, which is prone to react in the presence of atmospheric CO_2 during the slow drying at a relatively low temperature. Derevschikov et al. [17] also observed that this crystalline phase was obtained by using KOH as a precursor.

3.2. Reactivity and CO_2–H_2O capture capacity of supports and solid sorbents

First, to elucidate any possible reaction between the supports or impregnated absorbents with water vapor, the series of prepared materials were exposed to different conditions of relative humidity within the range of 0 to 80% and a constant temperature of 60 °C using N_2 as the carrier gas. Fig. 6 shows the water vapor adsorption/desorption isotherms, which were

generated as a function of the relative humidity (RH%). All of these adsorption isotherms show weight increases (in the adsorption stage) ranging from approximately 10.1 wt%, in the case of the A-Tween-10K sample, to approximately 73.7 wt%, registered for the A-Tween-40K sample. After that, during the desorption stage, sorption hysteresis was observed; however, in the case of the A-Tween and A-Tween-10K samples, the hysteresis loops tended to practically close, indicating that a reversible process took place and the weight increases observed during the adsorption stage were only due to physisorbed water condensation. On the other hand, despite the fact that the A-Tween-20K and A-Tween-40K samples showed similar behavior during desorption, the hysteresis loops did not close any further; therefore, a final mass gain of 5.1 and 8.4 wt% for samples A-Tween-20K and A-Tween-40K, respectively, was registered. This fact was attributed to the formation of the more hydrated carbonate species of $K_2CO_3 \cdot 1.5H_2O$ from the K_2CO_3 present in the untreated sorbent, as well as the presence of chemisorbed water due to the enhancement of the hydrophilic properties of the sorbent as a result of the presence of higher amounts of carbonate in the samples.

CO_2 sorption tests in the presence of water vapor were conducted at different RH% values and at temperatures of 60 and 80 °C. When sorbents were exposed to these temperatures and gas mixtures, a different behavior was observed during desorption, in comparison to the results observed when N_2–H_2O mixtures were used.

Fig. 7 shows the CO_2–water vapor adsorption/desorption isotherms, which were generated as a function of the relative humidity (0–80 RH %), at a temperature of 80 °C and using of pure CO_2 as the carrier gas. After the desorption stage, or in other words, when the system reached 0 RH%, a remarkable mass gain was observed. These results were attributed to the formation of $KHCO_{3(s)}$, according to reactions (A) and (B), and thus to carbonation. The absorption results that show the maximum mass
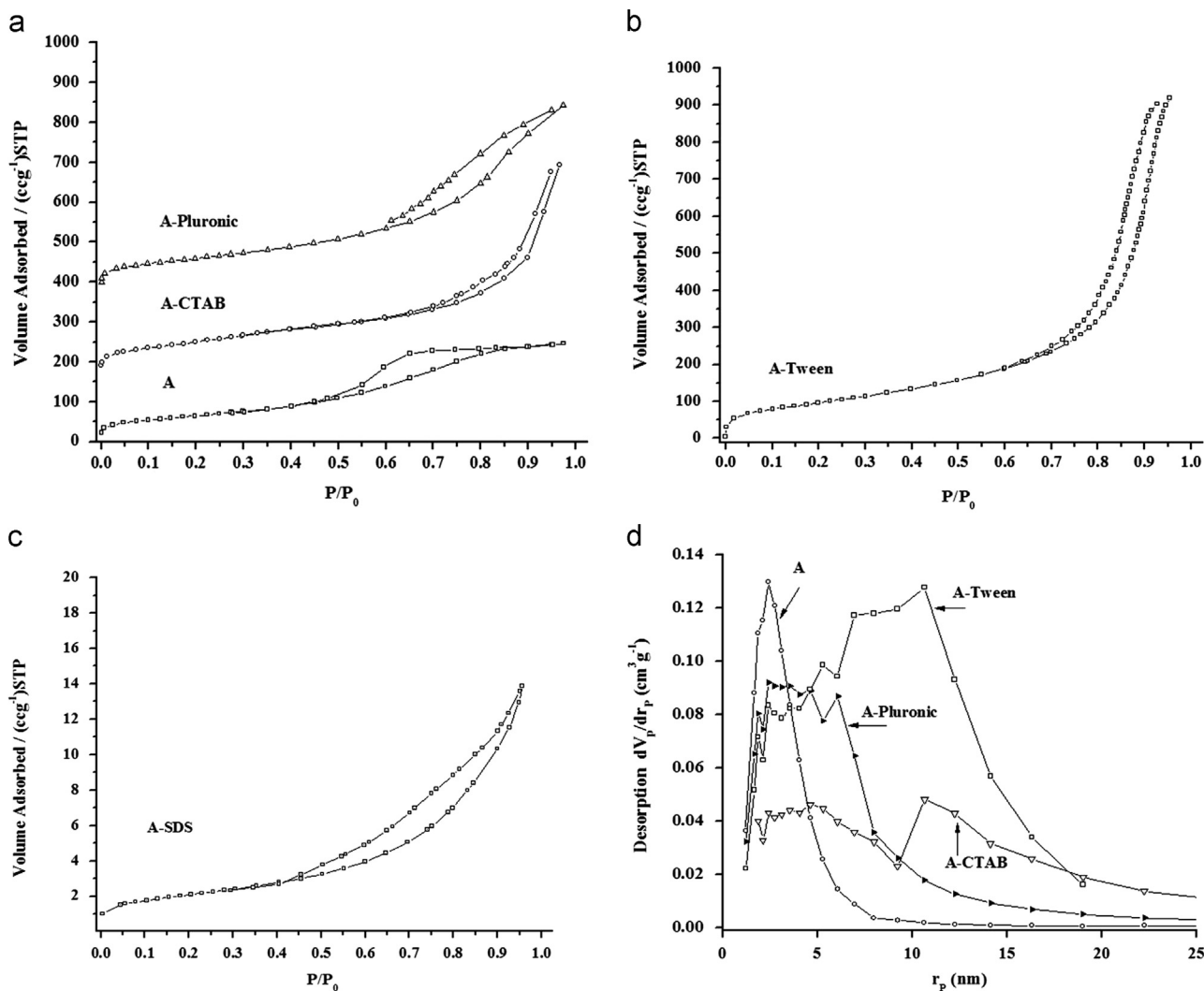
Fig. 3. (a)–(c) N_2 physisorption isotherms of supports prepared with different surfactants and (d) pore size distributions of the series of alumina supports. Pore sizes were estimated based on N_2 desorption isotherm applying the BJH method.

Table 2
Specific surface area values and chemical microanalysis of the series of sorbents prepared on A and A-Tween supports.

Sample	SSA_{BET} (m² g⁻¹)	K content (%wt) EDS analysis
A-20K	2.8	16.12
A-Tween	496.7	0.00
A-Tween-10K	127.9	4.47
A-Tween-20K	6.6	14.04
A-Tween-40K	0.22	29.01

gained after desorption are summarized in Table 3. The results presented in this table also reveal the effect of temperature. The total weight gain after desorption exhibited by the sorbents was higher in all of the cases when the sorption was performed at 80 °C, compared with that observed at 60 °C.

Based on the results, it is clear that the mass gain was proportional to the active phase loading present in the sorbents, as well as to temperature. Therefore, to verify that the mesostructured alumina support could provide additional advantages for

enhancing CO_2 absorption via an effective dispersion of potassium phases, the alumina support prepared with no surfactant added was also impregnated and tested as a CO_2 absorbent for comparison purposes.

Fig. 8 shows the CO_2–water vapor isotherms of the A-20K and A-Tween-20K samples, which were generated at 80 °C as a function of the relative humidity (RH%). The adsorption isotherms show the same primary adsorption/desorption behavior discussed before; however, it is clear that despite these two samples having almost the same potassium content (Table 2), the A-Tween-20K sample, or in other words, the sorbent prepared by using the high surface area support, exhibited a greater mass gain after desorption than the maximum mass gain observed for the A-20K sorbent. In fact, the final uptake difference was approximately 26% between these two samples. The results thus suggest that besides the potassium loading in the absorbent, which significantly affected the properties of CO_2 capture, the porosity of the support and other variables, such as temperature and the presence of moisture, also had a remarkable effect on the CO_2 capture properties of the resultant absorbents.
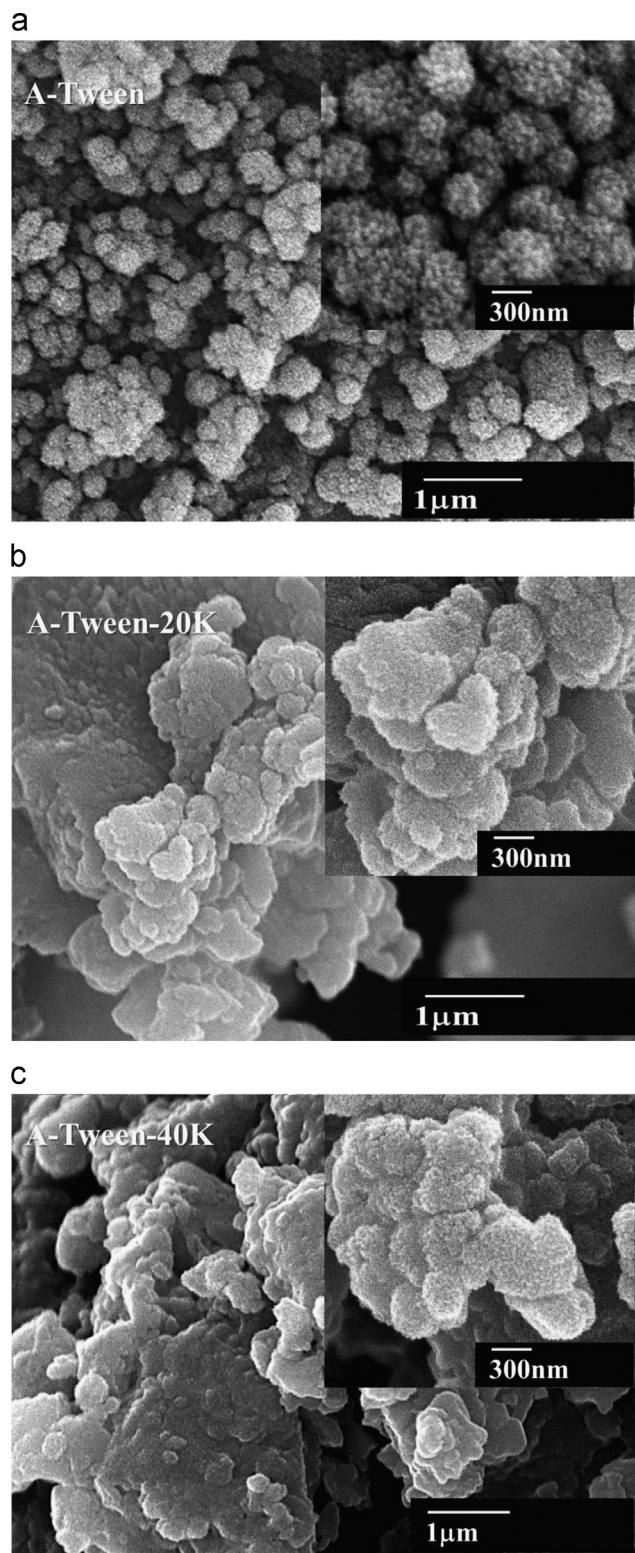
a

b

c

Fig. 4. SEM images of the A-Tween alumina support, A-Tween-20K and micrograph of A-Tween-40K sorbent.

Finally, it is important to mention that a deeper understanding of the effect of sorbent support on the uptake rate, as well as its performance during subsequent absorption-regeneration cycles, would lead to improvements in the CO_2
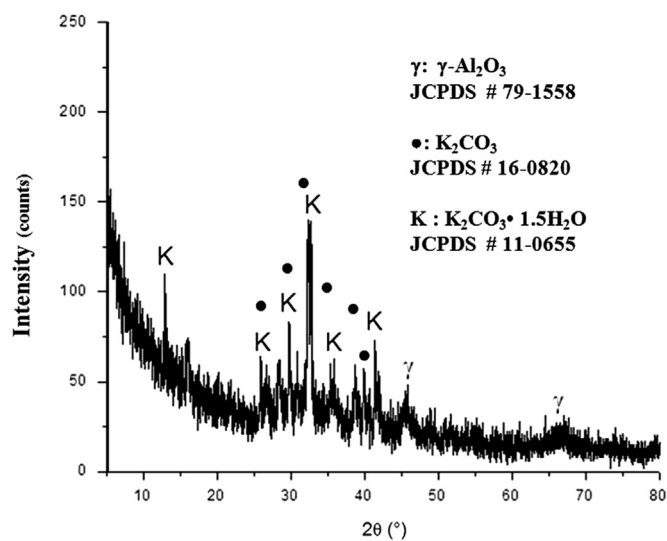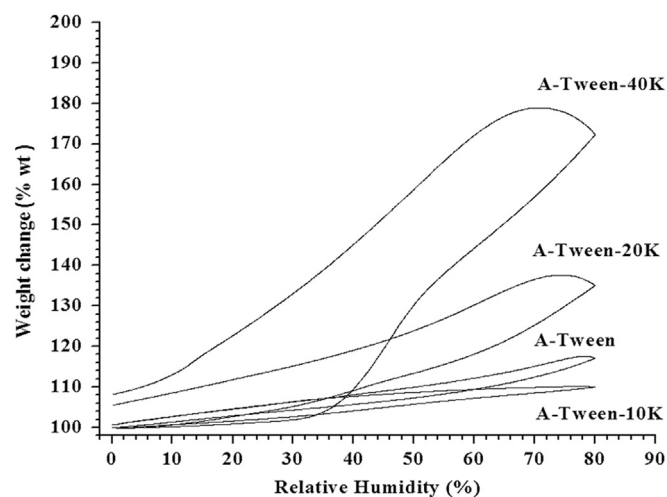

Fig. 5. XRD pattern of the A-Tween-40K sorbent.

Fig. 6. Isotherms of water adsorption/desorption at different relative humidity conditions under N_2 flow and temperature of 60 °C.
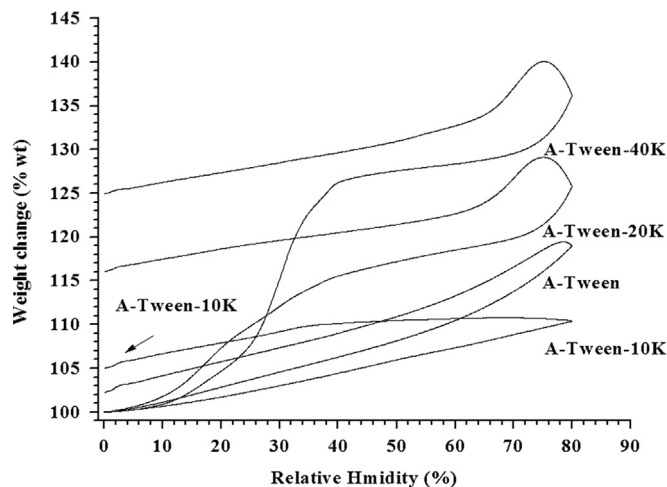

Fig. 7. Isotherms of CO_2–water adsorption/desorption at different relative humidity conditions under pure CO_2 flow and a temperature of 80 °C.

Table 3
Weight changes during CO_2–H_2O sorption for the different samples.

Sample	Total weight gain after desorption (wt%)			Maximum CO_2 sorption (mmol g^{-1})[a]
	N$_2$–H$_2$O atmosphere	CO$_2$–H$_2$O atmosphere		
	(60 °C)	(60 °C)	(80 °C)	(80 °C)
A-Tween	0.5	2	2	–
A-Tween-10K	0.5	3	5	0.80
A-Tween-20K	5.1	9	16	2.58
A-Tween-40K	8.4	21	25	4.03

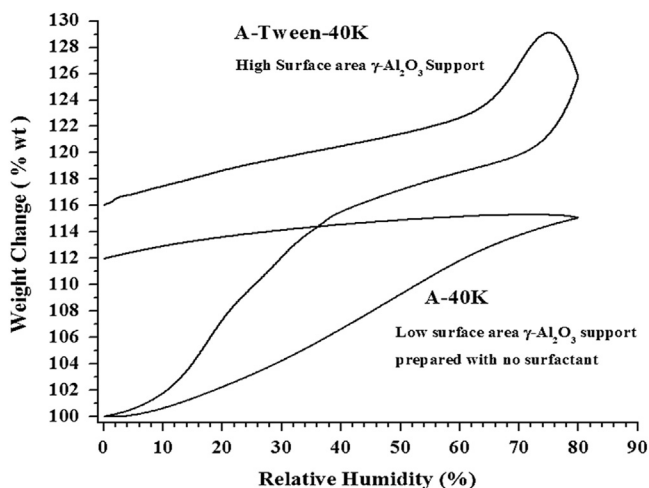[a]Based on the observed weight change.

Fig. 8. Isotherms of CO_2–water adsorption/desorption of A-20K and A-Tween 20K sorbents obtained at different relative humidity conditions under pure CO_2 flow and a temperature of 80 °C.

sorption capacity on these promising materials. Therefore, further studies regarding these sorbent properties will be conducted in future research.

4. Conclusions

Different mesoporous alumina materials were synthesized via the surfactant template method and then characterized structurally and microstructurally by different techniques. As it could be expected, samples presented high surface areas, as high as 496.7 m^2 g^{-1}. Thus, they were successfully used as supports for the preparation of K_2CO_3-based solid sorbents for the CO_2 capture.

Although the samples evidenced an important surface area and pore volume reduction after potassium impregnation, the sorbents showed excellent reactivity in the presence of CO_2–water vapor mixtures in the temperatures range of 60 to 80 °C. Results suggest that not only potassium loading but also temperature, moisture and the textural properties of mesostructured γ-Al_2O_3 supports have an effect on the absorption capacity of the sorbents. Additionally, as it could be expected, a better dispersion of

potassium active phases on the supports results in an enhancement of the CO_2 absorption process.

References

[1] M.E. Boot-Handford, J.C. Abanades, E.J. Anthony, M.J. Blunt, S. Brandani, N. Mac Dowell, J.R. Fernández, M. Chiara Ferrari, R. Gross, J.P. Hallett, R.S. Haszeldine, P. Heptonstall, A. Lyngfelt, Z. Makuch, E. Mangano, R.T.J. Porter, M. Pourkashanian, G.T. Rochelle, N. Shah, J.G. Yaoa, P.S. Fennell, Carbon capture and storage update, Energy Environ. Sci. 7 (2014) 130–189.
[2] Brett P. Spigarelli, S. Komar Kawatra, Opportunities and challenges in carbon dioxide capture, J. CO$_2$ Util. 1 (2013) 69–87.
[3] Lei Li, Ning Zhao, Wei Wei, Yuhan Sun, A review of research progress on CO$_2$ capture, storage, and utilization in Chinese Academy of Sciences, Fuel 108 (2013) 112–130.
[4] Q. Wang, J. Luo, Z. Zhong, A. Borgna, CO$_2$ capture by solid adsorbents and their applications: current status and new trends, Energy Environ. Sci. 4 (2011) 42–55.
[5] A.M. López-Periago, J. Fraile, P. López-Aranguren, L.F. Vega, C. Domingo, CO$_2$ capture efficiency and carbonation/calcination kinetics of micro and nanosized particles of supercritically precipitated calcium carbonate, Chem. Eng. J. 226 (2013) 357–366.
[6] M. Mohammadi, P. Lahijani, Abdul Rahman Mohamed, Refractory dopant-incorporated CaO from waste eggshell as sustainable sorbent for CO$_2$ capture: experimental and kinetic, Chem. Eng. J 243 (2014) 455–464.
[7] Shao Yun Shan, Qing Ming Jia, Li Hong Jiang, Qin Chao Li, Ya Ming Wang, Jin Hui Peng, Novel Li$_4$SiO$_4$-based sorbents from diatomite for high temperature CO$_2$ capture, Ceram. Int. 39 (5) (2013) 5437–5441.
[8] Seung Ju Han, Yongju Bang, Hyuk Jae Kwon, Hyun Chul Lee, Vishwanath Hiremath, In Kyu Song, Jeong Gil Seo, Elevated temperature CO$_2$ capture on nano-structured MgO–Al$_2$O$_3$ aerogel: effect of Mg/Al molar ratio, Chem. Eng. J. 242 (2014) 357–363.
[9] S.D. Angeli, C.S. Martavaltzi, A.A. Lemonidou, Development of a novel-synthesized Ca-based CO$_2$ sorbent for multicycle operation: parametric study of sorption, Fuel 127 (2014) 62–69.
[10] M. Zhao, M. Bilton, A.P. Brown, A.M. Cunliffe, E. Dvinino, V. Dupont, T.P. Comyn, S.J. Milne, Durability of CaO–CaZrO$_3$ sorbents for high temperature CO$_2$ capture prepared by a wet chemical method, Energy Fuels (2014), http://dx.doi.org/10.1021/ef4020845.
[11] Thongthai Witoon, Characterization of calcium oxide derived from waste eggshell and its application as CO$_2$ sorbent, Ceram. Int. 37 (8) (2011) 3291–3298.
[12] S. Wang, S. Yan, X. Ma, J. Gong, Recent Advances in capture of carbon dioxide using alkali-metal-based oxides, Energy Environ. Sci. 4 (2011) 3805–3819.
[13] M.J. Ramírez-Moreno, I.C. Romero-Ibarra, J. Ortiz-Landeros, H. Pfeiffer, Alkaline and alkaline-earth ceramic oxides for CO$_2$ capture, separation and subsequent catalytic chemical conversion, in: Claudia do Rosario Vaz Morgado, Victor Paulo Pecanha Esteves (Eds.), CO$_2$ Sequestration and Valorization, InTech Open Acces, 2014.
[14] Joong Beom Lee, Tae Hyoung Eom, Bok Seok Oh, Jeom-In Baek, Jungho Ryu, Won Sik Jeon, Young Ho Wi, Chong Kul Ryu, CO$_2$ capture from flue gas using potassium-based dry regenerable sorbents, Energy Procedia 4 (2011) 1494–1499.
[15] J.V. Veselovskaya, V.S. Derevschikov, T.Yu. Kardasha, O.A. Stonkusa, T.A. Trubitsinad, A.G. Okuneva, Direct CO$_2$ capture from ambient air

using K_2CO_3/Al_2O_3 composite sorbent, Int. J. Greenhouse Gas Control 17 (2013) 332–340.

[16] Soo Chool Lee, Ho Jin Chae, Soo Jae Lee, Yong Hee Park, Chong Kul Ryu, Chang Keun Yi, Jae Chang Kim, Novel regenerable potassium-based dry sorbents for CO_2 capture at low temperatures, J. Mol. Catal. B: Enzym. 56 (2009) 179–184.

[17] V.S. Derevschikov, J.V. Veselovskaya, T. Yu. Kardash, D.A. Trubitsyn, A.G. Okunev, Direct CO_2 capture from ambient air using K_2CO_3/Y_2O_3 composite sorbent, Fuel 127 (2014) 212–218.

[18] A. Goeppert, M. Czaun, G.K. Surya Prakash, G.A. Olah, Air as the renewable carbon source of the future: an overview of CO_2 capture from the atmosphere, Energy Environ. Sci. 5 (2012) 7833–7853.

[19] M. Mahmoudakhani, D.W. Keith, Low energy sodium hydroxide recovery for CO_2 capture from atmospheric air- thermodynamic analysis, Int. J. Greenhouse Gas Control 3 (2009) 376–384.

[20] V. Nikulshina, D. Hirsch, M. Mazzotti, A. Steinfeld, CO_2 capture from air and coproduction of H_2 via the $Ca(OH)_2$–$CaCO_3$ cycle using concentrated solar power: thermodynamic analysis, Energy 31 (2006) 1715–1725.

[21] W. Zhao, G. Sprachmann, Z. Li, N.i. Cai, X. Zhang, Effect of K_2CO_3–$1.5H_2O$ on the regeneration energy consumption of potassium-based sorbents for CO_2 capture, Appl. Energy 112 (2013) 381–387.

[22] A.G. Okunev, V.E. Sharonov, Yu.I. Aristov, V.N. Parmon, Sorption of carbon dioxide from wet gases by K_2CO_3 in porous matrix: influence of the matrix nature, React. Kinet. Catal. Lett. 71 (2) (2000) 355–362.

[23] Marcin Broda, Christoph R. Müller, Sol–gel-derived, CaO-based, ZrO_2-stabilized CO_2 sorbents, Fuel 127 (2014) 94–100.

[24] M. Hashem Sedghkerdar, Nader Mahinpey, Zhenkun Sun, Serge Kaliaguine, Novel synthetic sol–gel CaO based pellets using porous mesostructured silica in cyclic CO_2 capture process, Fuel 127 (2014) 101–108.

[25] Soo Chool Lee, Bo Yun Choi, Tae Jin Lee, Chong Kul ryu, Young Soo Ahn, Jae Chang Kim, CO_2 absorption and regeneration of alkali metal-based solid sorbents, Catal. Today 111 (2006) 385–390.

[26] Soo Chool Lee, Yong Mok Kwon, Suk Yong Jung, Joong Beom Lee, Chong Kul Ryu, Jae Chang Kim, Excellent thermal stability of potassium-based sorbent using ZrO_2 for post combustion CO_2 capture, Fuel 115 (2014) 97–100.

[27] Chuanwen Zhao, Yafei Guo, Changhai Li, Shouxiang Lu, Removal of low concentration CO_2 at ambient temperature using several potassium-based sorbents, Appl. Energy 124 (2014) 241–247.

[28] V.S. Derevschikov, J.V. Veselovskaya, T.Yu. Kardasha, D.A. Trubitsyn, A.G. Okuneva, Direct CO_2 capture from ambient air using K_2CO_3/Y_2O_3 composite sorbent, Int. J. Greenhouse Gas Control 17 (2013) 332–340.

[29] Soo Chool Lee, Yong Mok Kwon, Ho Jin Chae, Suk Yong Jung, Joong Beom Lee, Chong Kul Ryu, Chang Keun Yi, Jae Chang Kim, Improving regeneration properties of potassium-based alumina sorbents for carbon dioxide capture from flue gas, Fuel 104 (2013) 882–885.

[30] L.D. Bonifacio, B.V. Lotsch, G.A. Ozin, Periodic mesoporous materials: holes filled with opportunities, Compre. Nanosci. Technol. 5 (2011) 69–125.

[31] N.R. Stuckert, R.T. Yang, CO_2 capture from the atmosphere and simultaneous concentration using zeolites and amine-grafted SBA-15, Environ. Sci. Technol. 45 (23) (2011) 10257–10264.

[32] M.B. Yue, L.B. Sun, Y. Cao, Y. Wang, Z.J. Wang, J.H. Zhu, Efficient CO_2 capturer derived from as-synthesized MCM-41 modified with amine (—A Eur. J.), Chemistry 14 (11) (2008) 3442–3451.

[33] A. Heydari-Gorgi, Y. Belmabkhout, A. Sayari, Polyethylenimine-impregnated mesoporous silica: effect of amine loading and surface alkyl chains on CO_2 adsorption, Langmuir 27 (20) (2011) 12411–12416.

[34] K. Wörmeyer, I. Smirnova, Adsorption of CO_2, moisture and ethanol at low partial pressure using aminofunctionalised silica aerogels, Chem. Eng. J. 225 (2013) 350–357.

[35] J. Wang, H. Chen, H. Zhou, X. Liu, W. Qiao, D. Long, et al., Carbon dioxide capture using polyethylenimine-loaded mesoporous carbons, J. Environ. Sci. 25 (1) (2013) 124–132.

[36] Q. Ye, J. Jiang, C. Wang, Y. Liu, H. Pan, Y. Shi, Adsorption of low-concentration carbon dioxide on amine-modified carbon nanotubes at ambient temperature, Energy Fuels 26 (2012) 2497–24504.

[37] S. Kumar, S.K. Saxena, A comparative study of CO_2 sorption properties for different oxides, Mater. Renewable Sustainable Energy Rev. 3 (2014) 30, http://dx.doi.org/10.1007/s40243-014-0030-9.

[38] Seul-Yi Lee, Soo-Jin Park, A review on solid adsorbents for carbon dioxide capture, J. Ind. Eng. Chem. (2014), http://dx.doi.org/10.1016/j.jiec.2014.09.001.

[39] J. Wang, L. Huang, R. Yang, Z. Zhang, J. Wu, Y. Gao, Q. Wang, D. OHare, Z. Zhong, Recent advances in solid sorbents for CO_2 capture and new development trends, Energy Environ. Sci. (2014), http://dx.doi.org/10.1039/C4EE01647E.

[40] Chang Liu, Yongchun Liu, Qingxin Ma, Hong He, Mesoporous transition alumina with uniform pore structure synthesized by alumisol spray pyrolysis, Chem. Eng. J. 163 (2010) 133–142.

[41] L. Samain, A. Jaworski, M. Edén, D.M. Ladd c, Dong-Kyun Seo, F.J. García-García, Ulrich Häussermann, Structural analysis of highly porous γ-Al_2O_3, J. Solid State Chem. 217 (2014) 1–8.

[42] S. Lowell, J.E. Shields, M.A. Thomas, Characterization of porous solids and powders: surface area, pore size an density, Particle Technology Series, Kluwer Academic Publishers, London, 2004.